Adaptive $\mathcal{C}h$ method with Local Coupled Multiquadrics for Partial Differential Equations

Ahmed E. Seleit

Senior Engineer, ASML

Lecturer, Mechanical Engineering, Johns Hopkins University

Abstract

We present a new adaptive collocation scheme for solving partial differential equations based on Local Coupled Multiquadrics (LCMQs) within a covers-and-nodes framework. The method, referred to as the Adaptive $\mathcal{C}h$ Method, automatically adjusts the cover size $\mathcal{C}$ and refines local nodal spacing h to meet a prescribed tolerance. Numerical examples for one- and two-dimensional Poisson problems demonstrate accurate solutions across a range of shape parameter values, while preserving the advantages of local collocation. The proposed approach is a truly meshless method, requiring no element or connectivity/continuity to construct trial functions or weights.

1 Introduction

Radial-basis-function (RBF) [1] collocation has matured into a competitive meshless methodology for Partial Differential Equations (PDEs) [2–7]. Zhang [8,9] introduced *Coupled* RBFs (CRBFs) that reduce sensitivity to the shape parameter while preserving accuracy and stable conditioning. Moreover, the author highlighted that Coupled Multiquadrics (CMQs) demonstrated better stability and performance compared to its counterparts. In contrast to standard RBFs that demand careful tuning of the shape parameter to avoid instability or poor convergence [10–20], CRBFs remove this burden. Lee *et al.* [21] developed a *local* multiquadric framework in which a global banded matrix assembled on overlapping covers, thereby avoiding large dense global RBF gramians. For adaptivity, Patterson [22] proposed a principled *ph* strategy that favors increasing the polynomial order p then refining the nodal distance h based on interval-wise error indicators that has proven effective in pseudo-spectral settings; the same decision logic can be transposed to local RBF setups.

In this work, we introduce a novel approach that integrates: (i) the concept of solving PDEs via Kansa method and CMQs, with (ii) the idea of local RBF covers, and (iii) adaptivity inspired by the ph-refinement method developed for optimal control. In this approach, we automatically adjust the cover size $\mathcal{C}$ and refine the nodal distance h to accurately solve PDEs. We refer to this integrated approach as the Adaptive $\mathcal{C}h$ method. We demonstrate this approach on 1D and 2D Poisson problems with Dirichlet boundary conditions. The demonstration shows that the method achieves the required tolerance and exhibits low sensitivity to variations in the shape parameter.

2 LCMQ Covers

Let $\Omega \subset \mathbb{R}^d$ be a bounded domain with boundary $\partial\Omega$ and $X = \{x_i\}_{i=1}^N \subset \Omega$ be distinct nodes. We seek $u : \Omega \to \mathbb{R}$ that satisfies

$$\mathcal{L}u(x) = f(x), \quad x \in \Omega, \qquad \mathcal{B}u(x) = g(x), \quad x \in \partial\Omega, \tag{1}$$

where $\mathcal{L}$ is a linear differential operator and $\mathcal{B}$ collects Dirichlet/Neumann boundary operators. We denote by u_h the meshless local–CRBF approximant introduced below.

For each node x_i, we associate a finite *cover* $\Omega_{x_i} = \{x_{i_j}\}_{j=1}^{\mathcal{C}_i} \subset X$ of cardinality $\mathcal{C}_i$, typically chosen as the $\mathcal{C}_i$ nearest neighbors of x_i. Let $\rho_i := \max_{x_{i_j} \in \Omega_{x_i}} \|x_{i_j} - x_i\|$ and $B_i := \{x \in \Omega : \|x - x_i\| \le \rho_i\}$. The collection of covers is *admissible* if (i) each target point involved in collocation belongs to at least one cover and (ii) the union of cover regions embraces the domain:

$$\Omega \;=\; \bigcup_{i=1}^{N} B_i, \qquad x \in \Omega \iff \exists\, i :\; x \in B_i. \tag{2}$$

Local support The local approximation at a target point x uses only the nodal values from Ω_{x_i}, i.e. its support is restricted to the chosen cover. Note that covers generally overlap: a node x_j may belong to several covers Ω_{x_i}, leading to a sparse but globally coupled system. Let $\phi(r; c)$ denote a CRBF with shape parameter $c > 0$, where $r = \|x - x_{i_j}\|$ is the distance between x and a cover node $x_{i_j} \in \Omega_{x_i}$. In this work, we adopt the coupled multiquadric (CMQ) [8],

$$\phi_{\mathrm{CMQ}}(r; c) \;=\; \sqrt{1 + \big(r/c\big)^2} \;+\; r^5. \tag{3}$$

Let $U_i \in \mathbb{R}^{\mathcal{C}_i \times \mathcal{C}_i}$ be the local kernel matrix, $(U_i)_{j\ell} = \phi_{\mathrm{CMQ}}(\|x_{i_j} - x_{i_\ell}\|; c)$, where $j, \ell = 1, \ldots, \mathcal{C}_i$. Let

$$\psi_i(x) \;=\; \big[\phi_{\mathrm{CMQ}}(\|x - x_{i_1}\|; c), \ldots, \phi_{\mathrm{CMQ}}(\|x - x_{i_{\mathcal{C}_i}}\|; c)\big]^\top. \tag{4}$$

The local shape vector is $W_i(x) = U_i^{-1}\psi_i(x)$ and the approximation (restricted to the union of covers) is

$$u_h(x) \;=\; \sum_{j=1}^{\mathcal{C}_i} W_{i,j}(x)\, u(x_{i_j}). \tag{5}$$

At interior collocation points x_i, we enforce $\mathcal{L}u = f$ by

$$\sum_{j \in \Omega_{x_i}} \big(\mathcal{L}W_{i,j}\big)(x_i)\, u(x_j) \;=\; f(x_i). \tag{6}$$

Let $\mathcal{L}$ be any second-order linear differential operator acting on x (e.g. the Laplacian). Since U_i is independent of x, we have $(\mathcal{L}W_i)(x) = U_i^{-1}(\mathcal{L}\psi_i)(x)$. Hence,

$$\sum_{j \in \Omega_{x_i}} \big(\mathcal{L}W_{i,j}\big)(x_i)\, u(x_j) = \sum_{j=1}^{\mathcal{C}_i} \Big[\, U_i^{-1}\, (\mathcal{L}\psi_i)(x_i) \,\Big]_j\, u(x_{i,j}) \;=\; f(x_i), \tag{7}$$

where $(\mathcal{L}\psi_i)(x)$ is defined component-wise by $\big((\mathcal{L}\psi_i)(x)\big)_j = \mathcal{L}\big[\phi(\|x - x_{i,j}\|; c)\big]$. Boundary data are imposed directly. This procedure yields a sparse, banded global system.

3 Adaptive $\mathcal{C}h$ Method on LCMQ Covers

We present the Adaptive $\mathcal{C}h$ method on a generic domain $\Omega \subset \mathbb{R}^d$. We employ a simple logic: when the a posteriori indicator is unacceptable, first attempt $\mathcal{C}$-enrichment; if insufficient, perform h-refinement by inserting nodes.

Residual-type indicator. Let $\{K_g\}_{g=1}^{G}$ be a nonoverlapping partition of Ω into *marker cells* used only for error estimation and node insertion. Denote the cell diameter by $h_g := \mathrm{diam}(K_g)$ and its center by ζ_g. For a baseline cover size $\mathcal{C}$, define an *enriched* solution u_h^{enr} obtained by using cover size $C + \Delta p$, where Δp is a small integer, when evaluating the residual. The error indicator on K_g is

$$\mathscr{E}_g \;=\; h_g^2 \,\big|(\mathcal{L}u_h^{\mathrm{enr}})(\zeta_g) - f(\zeta_g)\big|. \tag{8}$$

We also permit a classifier

$$s_g \;=\; h_g^2 \,\big|(\mathcal{L}u_h^{\mathrm{enr}} - \mathcal{L}u_h^{\mathrm{base}})(\zeta_g)\big|, \tag{9}$$

to bias the decision toward p or h-refinement. This is a *truly meshless method* because our approximation spaces are constructed from node clouds via local CMQ kernels; no element mesh or connectivity/continuity is used to define trial functions or weights. K_g is employed only for error marking and node insertion, which is an auxiliary device and does not affect the meshless construction. The adaptive cycle is further explained in Algorithm 1.

Algorithm 1 Generic-d Local–CRBF ph-Adaptive Collocation

Require: domain $\Omega \subset \mathbb{R}^d$; initial nodes $X^{(0)}$; CMQ shape c; cover cardinality bounds $n_{\min}, n_{\max}$; tolerance τ; max splits per cycle M; fraction of bad cells trigger $\theta \in (0,1)$; enrichment step Δp; adaptive cycle $k = 0, 1, 2, \ldots, \mathscr{K}$.

$\mathscr{K} \leftarrow 0$, $k \leftarrow 0$; **initialize per-cover sizes** $\mathcal{C}_i \leftarrow n_{\min}$ for all nodes $x_i \in X^{(0)}$.
repeat
  Assemble and solve the local–CRBF system on $X^{(k)}$ with **per-node cover sizes** $\{\mathcal{C}_i\}$ to obtain $u_h^{(k)}$ [21].
  For each marker cell K_g, compute $\mathscr{E}_g$ and s_g at its center ζ_g using **enriched per-node sizes** $\{\mathcal{C}_i + \Delta p\}$ *for evaluation only.*
  if $\dfrac{\big|\{g : \mathscr{E}_g > \tau\}\big|}{G} \geq \theta$ **and** $(\exists\, i : \mathcal{C}_i < n_{\max})$ **then** ▷ local p-refinement (per-cover)
    Let $\mathcal{G} \leftarrow \{g : \mathscr{E}_g > \tau\}$ (marked cells).
    for all $K_g \in \mathcal{G}$ **do**
      for all nodes $x_i \in K_g$ **do**
        $\mathcal{C}_i \leftarrow \min\{\, \mathcal{C}_i + \Delta p,\ n_{\max} \,\}$ ▷ increase p only where needed
      end for
    end for
    $X^{(k+1)} \leftarrow X^{(k)}$ ▷ no new nodes in p-step
  else ▷ h-refinement fallback
    Insert cell centers for up to the M worst cells ($\mathscr{E}_g$ largest):
      $X^{(k+1)} \leftarrow X^{(k)} \cup \{\text{selected } \zeta_g\}$.
    Initialize $\mathcal{C}_i \leftarrow n_{\min}$ for each newly inserted node; keep existing $\{\mathcal{C}_i\}$ unchanged.
  end if
  Enforce caps on $|X^{(k+1)}|$ and on all $\mathcal{C}_i \in [n_{\min}, n_{\max}]$.
  $k \leftarrow k + 1$.
until $\max_g \mathscr{E}_g \leq \tau$ or $k = \mathscr{K}$.

4 Numerical Experiments

We assess the accuracy and robustness of the proposed method on canonical Poisson problems in one and two dimensions. Throughout, u denotes the exact solution and u_h the numerical approximation obtained on the current node set and covers. To avoid nodal bias, errors are evaluated on an independent uniform probe set $\mathcal{P} = \{z_m\}_{m=1}^{M} \subset \Omega$. The *absolute error* at a point $z \in \Omega$ is

$$e(z) \;=\; \big|\, u(z) - u_h(z) \,\big|,$$

and the reported global error is the *root-mean-square error* (RMSE),

$$\mathrm{RMSE} \;=\; \left(\frac{1}{M} \sum_{m=1}^{M} \big|\, u(z_m) - u_h(z_m) \,\big|^2 \right)^{1/2}.$$

Plots will show either the point-wise absolute error $e(z)$ or the aggregate RMSE versus iteration, node count, or cover size, as appropriate.

Example 1: 1D Poisson, Dirichlet

Find $u : [-1, 1] \to \mathbb{R}$ such that

$$u''(x) = \frac{105}{2}x^2 - \frac{15}{2}, \qquad u(-1) = u(1) = 1. \tag{10}$$

The exact solution is

$$u^\star(x) = \frac{35}{8}x^4 - \frac{15}{4}x^2 + \frac{3}{8}. \tag{11}$$

In the 1D implementation, we evaluate midpoint indicators with an enriched cover of size $n+\Delta p$. We use the decision policy in Algorithm 1 and the solver settings in Table 1. The adaptive solver progressively decreases the error as shown in Figure 1c and achieves the tolerance after 11 cycles. Moreover, it changed the number of nodes to 50 and the cover size to 19 at the terminal cycle. We show that the maximum absolute error is below the chosen tolerance in Figure 1b. This local adaptive method works with varying accuracy for variation in the shape parameter compared to classic RBFs that would not converge at most of the shape parameter values displayed in 1d.

Table 1: Solver configuration for Examples 1 and 2

Parameter (symbol)	**Values in Example 1**	**Values in Example 2**
Domain $[a, b]$	$[-1,\ 1]$	$[0,\ 1], [0,\ 1]$
Nodes N_0	40	17×17
Cover size $\mathcal{C}_0$	5	5
Shape parameter c	0.7	0.8
Residual tol. τ	6×10^{-5}	10^{-5}

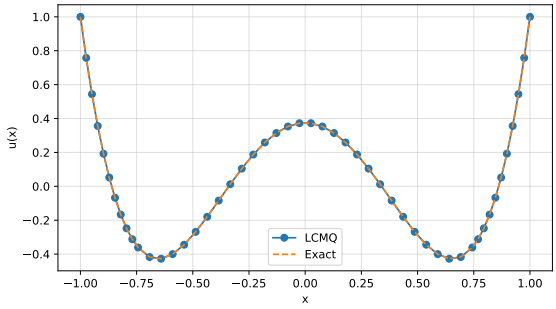

(a) Numerical Vs Exact values of u of the 1D Poisson

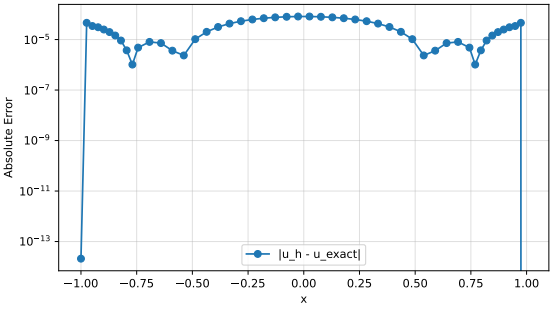

(b) Absolute error $|u_h - u|$over the domain $[-1, 1]$

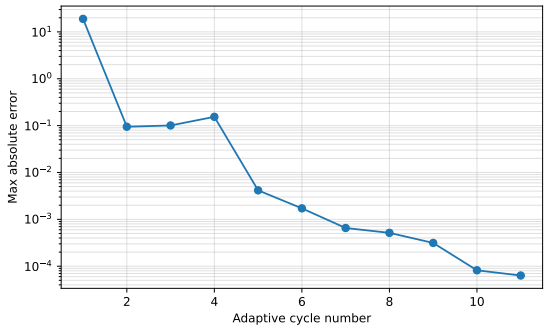

(c) Maximum absolute error Vs Cycle number

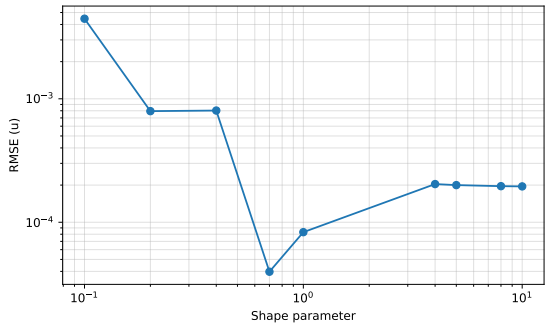

(d) RMSE Vs variation in the shape parameter

Figure 1: Solution of the 1D Poisson example.

Example 2: Poisson on the unit square, Dirichlet

The extension to 2D problems is straightforward. For a set of nodes $\{x_i, y_i\}_{i=1}^{N} \subset \Omega \subset \mathbb{R}^2$, each cover $\Omega_{(x_i,y_i)}$ is formed by selecting the nearest $\mathcal{C}_i$ neighbors of the center node (x_i, y_i). The radius measured from a query point (x, y) is described as $r = \sqrt{(x - x_{i_j})^2 + (y - y_{i_j})^2}$. Logic similar to that in Algorithm1 is adopted.

Now, let $\Omega = [0, 1]^2$. it is required to find $u : \Omega \to \mathbb{R}$ such that

$$\nabla^2 u(x, y) = \sin(\pi x) \sin(\pi y), \qquad u|_{\partial\Omega} = 0. \tag{12}$$

The exact solution is

$$u^\star(x, y) = -\frac{1}{2\pi^2} \sin(\pi x) \sin(\pi y). \tag{13}$$

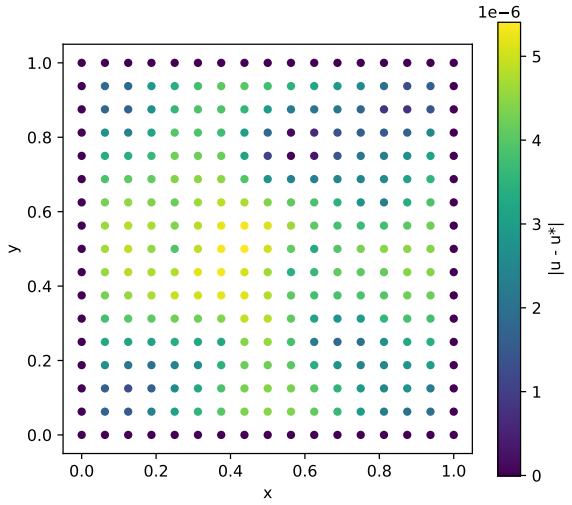

Figure 2: Numerical solution and Absolute error of the 2D Poisson.

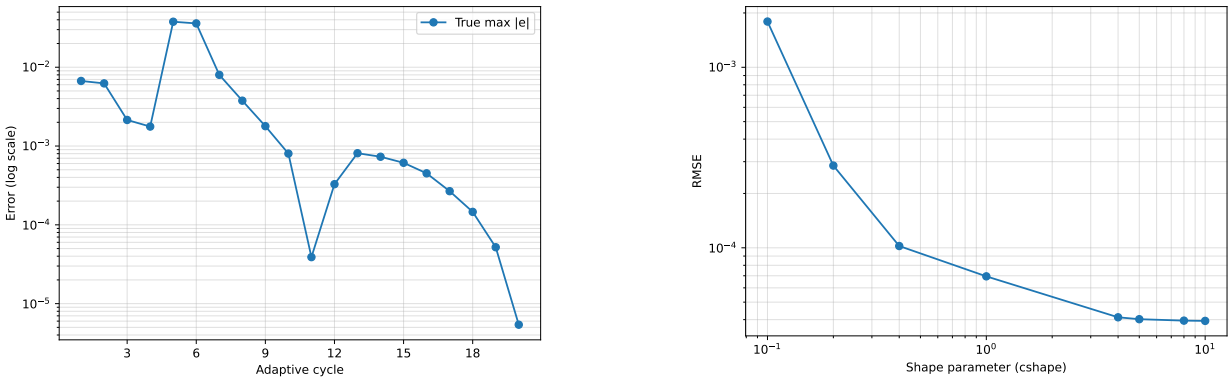

(a) True error vs Adaptive Cycle Number.

(b) RMSE vs variation in the shape parameter.

Figure 3: Error in the 2D Poisson example.

Adaptive LCMQ achieves good accuracy, as shown in 2, well below the set tolerance described in Table1. Moreover, it stopped after 20 cycles with RMSE in the order of 10^{-5} as presented in Figure3, favoring cover sizes change (up to to 43) over local nodal refinement. The LCMQ solution does not blow up for various values of the shape parameter in Figure 3b.

5 Conclusions

We extended the global CMQ method to a local one within an adaptive framework that remains truly meshless. The method inherits the desirable shape-parameter low sensitivity of CMQs while operating with banded matrices. The simple adaptive *ph* logic, choosing when to grow cover sizes and when to insert nodes locally, shows good accuracy. Benchmarks suggest that LCMQ collocation offers a reliable, scalable pathway to BVPs with reduced sensitivity to c.

Declaration of generative AI and AI-assisted technologies in the writing process During the preparation of this work the author(s) used "Overleaf embedded AI Assistance and Writeful" in order to proofread and ensure language coherence across the article. After using this tool/service, the author(s) reviewed and edited the content as needed and take(s) full responsibility for the content of the publication.

References

[1] M. D. Buhmann, "Radial basis functions," *Acta numerica*, vol. 9, pp. 1–38, 2000.

[2] G. E. Fasshauer, *Meshfree approximation methods with Matlab (With Cd-rom)*, vol. 6. World Scientific Publishing Company, 2007.

[3] E. J. Kansa, "Multiquadrics—a scattered data approximation scheme with applications to computational fluid-dynamics—ii solutions to parabolic, hyperbolic and elliptic partial differential equations," *Computers & mathematics with applications*, vol. 19, no. 8-9, pp. 147–161, 1990.

[4] M. Jankowska, A. Karageorghis, and C. Chen, "Kansa rbf method for nonlinear problems," *Boundary Elements and Other Mesh Reduction Methods*, p. 39, 2018.

[5] H. Mirinejad and T. Inanc, "An rbf collocation method for solving optimal control problems," *Robotics and Autonomous Systems*, vol. 87, pp. 219–225, 2017.

[6] A. E. Seleit and T. A. Elgohary, "A shape parameter insensitive crbfs-collocation for solving nonlinear optimal control problems," *Optimal Control Applications and Methods*, vol. 45, no. 1, pp. 413–435, 2024.

[7] T. Elgohary, L. Dong, J. Junkins, and S. Atluri, "A simple, fast, and accurate time-integrator for strongly nonlinear dynamical systems," *CMES: Computer Modeling in Engineering & Sciences*, vol. 100, no. 3, pp. 249–275, 2014.

[8] Y. Zhang, "An accurate and stable rbf method for solving partial differential equations," *Applied Mathematics Letters*, vol. 97, pp. 93–98, 2019.

[9] C. Zhang, Z. Fu, and Y. Zhang, "A novel global rbf direct collocation method for solving partial differential equations with variable coefficients," *Engineering Analysis with Boundary Elements*, vol. 160, pp. 14–27, 2024.

[10] B. Fornberg and G. Wright, "Stable computation of multiquadric interpolants for all values of the shape parameter," *Computers & Mathematics with Applications*, vol. 48, no. 5–6, pp. 853–867, 2004.

[11] B. Fornberg, E. Lehto, and C. Powell, "Stable calculation of gaussian-based rbf–fd stencils," *Computers & Mathematics with Applications*, vol. 65, pp. 627–637, 2013.

[12] G. B. Wright and B. Fornberg, "Stable computations with flat radial basis functions using vector-valued rational approximations," *Journal of Computational Physics*, vol. 331, pp. 137–156, 2017.

[13] A. H.-D. Cheng, "Multiquadric and its shape parameter—a numerical investigation of error estimate, condition number, and round-off error by arbitrary precision computation," *Engineering Analysis with Boundary Elements*, vol. 36, pp. 220–239, 2012.

[14] W. Chen, Y. Hong, and J. Lin, "The sample solution approach for determination of the optimal shape parameter in the multiquadric function of the kansa method," *Computers & Mathematics with Applications*, vol. 75, pp. 2942–2954, 2018.

[15] S. Rippa, "An algorithm for selecting a good value for the parameter c in the radial basis function interpolation," *Advances in Computational Mathematics*, vol. 11, pp. 193–210, 1999.

[16] L. Ling and R. Schaback, "An improved subspace selection algorithm for meshless collocation methods," *International Journal for Numerical Methods in Engineering*, vol. 80, pp. 1623–1639, 2009.

[17] S. A. Sarra and E. J. Kansa, "Multiquadric radial basis function approximation methods for the numerical solution of partial differential equations," *Advances in Computational Mechanics*, vol. 2, p. 206, 2009. Issue/volume information may require confirmation.

[18] F. Wang, W. Chen, C. Zhang, and Q. Hua, "Kansa method based on the hausdorff fractal distance for hausdorff derivative poisson equations," *Fractals*, vol. 26, p. 1850084, 2018.

[19] C.-S. Liu and D. Liu, "Optimal shape parameter in the mq-rbf by minimizing an energy gap functional," *Applied Mathematics Letters*, vol. 86, pp. 157–165, 2018.

[20] A. H.-D. Chen, D.-L. Young, and C.-C. Tsai, "Solution of poisson's equation by iterative drbem using compactly supported, positive definite radial basis function," *Engineering Analysis with Boundary Elements*, vol. 24, pp. 549–557, 2000.

[21] C. K. Lee, X. Liu, and S. C. Fan, "Local multiquadric approximation for solving boundary value problems," *Computational Mechanics*, vol. 30, no. 5, pp. 396–409, 2003.

[22] M. A. Patterson, W. W. Hager, and A. V. Rao, "A ph mesh refinement method for optimal control," *Optimal Control Applications and Methods*, vol. 36, no. 4, pp. 398–421, 2015.